Communications on Applied Electronics (CAE) – ISSN : 2394-4714
Foundation of Computer Science FCS, New York, USA
Volume 3– No.6, November 2015 – www.caeaccess.org

Study of the Effect of Excitation Frequency Variation on the Output of LVDT

Subhashis Maitra
Kalyani Government Engineering College
Kalyani, Nadia, West Bengal, India

ABSTRACT
Linear Variable Differential Transformer (LVDT) is a displacement transducer which found its widespread application in process industry for the measurement of flow [1], pressure [2], level [3] and temperature [4] in terms of displacement. LVDT is also used to measure force [5], velocity [6] etc. with a high degree of accuracy and reliability. It is well known that the output of LVDT varies linearly with the core motion based on some pre-assumption as mentioned in different literatures [1] – [8]. However the output is not perfectly linear because of the effect of the construction of the LVDT, material of the core; inter winding capacitance, stray capacitance and self inductances of the primary and secondary. Again the reactance of capacitance and inductance vary with the excitation frequency. Hence, though the output of LVDT is assumed linear with the excitation frequency, but in practice, it varies nonlinearly with the excitation frequency. In this paper, the effect of the excitation frequency on the output of LVDT has been studied and the outputs have been tabulated for the frequency range 50 Hz to 100 Hz. Also the variation of the output with frequency has been explained graphically.

Keywords
Capacitance, Excitation frequency, Inductances, LVDT, Transducer.

1. INTRODUCTION
Researchers have developed different types of displacement transducer in aspect of range of displacement, sensitivity, linearity and accuracy, like linear variable differential transformer (LVDT) [9], capacitive transducer [10], potentiometric transducer [11], resistive transducer [12], etc. Each of these transducers has its drawbacks and imperfections. LVDT is an electro-mechanical displacement transducer [9],[13], which has three coils namely one primary and two secondary. Current in the primary coil induces e.m.f. on the two secondary. The induced e.m.f. depends on the mutual inductances between the primary and the secondary of the LVDT. The mutual inductances again depend on the displacement of the core inside the LVDT and on the material of the core. The resulting output is the difference between the two e.m.f.s induced on both the secondary. The output of the LVDT is controlled by the position of the magnetic core. The two secondary of the LVDT are connected in opposition so that the output should be the difference between the two induced e.m.f. in the two secondary. At the centre of the position measurement stroke, the two secondary voltages of the displacement transducer are equal but because they are connected in opposition, the resulting output from the sensor is zero. As the LVDTs core moves away from centre, the result is an increase in one of the position sensor secondary and a decrease in the other. This results in an output from the measurement sensor. With LVDTs, the phase of the output (compared with the excitation phase) enables the electronics to know which half of the coil the core is in. Since there is no electrical contact across the transducer position sensing element, it offers many advantages over potentiometric linear transducers such as frictionless measurement, infinite mechanical life, excellent resolution and good repeatability. Its main disadvantages are its dynamic response and the effects of the exciting frequency. LVDT can also be used as a secondary transducer in various measurement systems. In those cases, a primary transducer is used to provide a displacement corresponding to the measurand and LVDT is then used to convert the measured displacement into corresponding electrical signal. In case of pressure measurement, displacement of a diaphragm or of the tip of a Bourdon tube is measured using LVDT [14]. Similarly in case of acceleration and force measurement, the displacement of an elastic element subjected to the given force is measured by LVDT [15]. However, the drawback of LVDT is its larger body length and its output is affected by stray magnetic field and excitation frequency as discussed in [16],[17]. To eliminate this error, Dhiman et.al discussed in [16], a strain gauge based displacement sensor that introduced mechanical error in terms of ruggedness. Where, displacement in the range of millimeter is to be measured, capacitive type transducer may be used to measure for its good frequency response. But the drawback of this type of transducer is its nonlinear behavior on account of edge effect and high output impedance on account of its low capacitance value. Hence in this case, the output varies with the excitation frequency resulting an erroneous result. Different literatures on LVDT so far studied, show the range of measurement, accuracy, reliability, fields of applications etc. but the variation of its output with frequency due to inter winding and stray capacitances has not been discussed so far. In this paper, the effect of stray and inter winding capacitance especially in low range displacement measurement has been discussed. The variations of the output of LVDT with different frequencies have been discussed in tabular form. The plots of the output with frequencies explore how and in which range a specific LVDT can be used with how much degree of accuracy.

Communications on Applied Electronics (CAE) – ISSN : 2394-4714
Foundation of Computer Science FCS, New York, USA
Volume 3– No.6, November 2015 – www.caeaccess.org

2. WORKING OF LVDT WITHOUT THE INTER WINDING CAPACITANCES

The equivalent circuit of an LVDT [1],[2] without considering the stray and inter winding capacitances is shown in Fig.1.

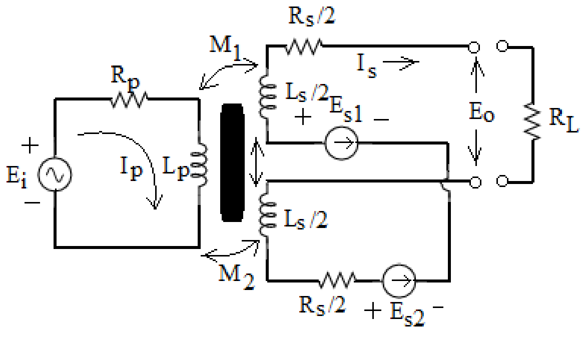

Fig. 1. Equivalent circuit of LVDT.

From Fig. 1, it is clear that the equation for the input, Ei and the output Eo, can be written as

$$Ei = IpRp + sLpIp \quad (1)$$

$$Eo = Es1 - Es2 = (M1 - M2)sIp \quad (2)$$

The difference (M1 – M2) varies with the core motion and if it is assumed that the difference varies linearly with the core motion, then it can be written as

M1 – M2 = kd, where ‘k’ is the proportionality constant and ‘d’ is the core displacement.

However, the frequency response of the LVDT as stated in [1] is

$$|E_o/E_i(j\omega)/d(j\omega)| = \frac{\omega k R_L/[R_p(R_S+R_L)]}{\sqrt{[\{1-\omega^2(\tau_m^2+\tau_p\tau_s)\}^2+\omega^2(\tau_p+\tau_s)^2]}} \quad (3)$$

and the phase angle difference between Eo and Ei is given by, $\theta = 90^0 - \tan^{-1}\frac{\omega(\tau_p+\tau_s)}{1-\omega^2(\tau_m^2+\tau_p\tau_s)}$ (4)

Where, $\tau_P = L_p/R_p$, $\tau_s = L_s/(R_s + R_L)$ and $\tau_m^2 = \frac{(M_1-M_2)^2}{\{R_p(R_s+R_L)\}}$. From (4), it is clear that, at frequency, $\omega = \frac{1}{\sqrt{\tau_m^2+\tau_p\tau_s}}$, the phase difference between the excitation voltage and the output is zero degree. Figure 2(a) and (b) show the variation of $E_o(j\omega)/d(j\omega)$ and phase angle with frequency respectively, considering Lp = 6 mH, Rp = 100 Ω, M1= 8 mH, M2 = 4 mH, LS = 4 mH, Rs = 100 Ω, RL = 200 Ω, d = 2 mm and Ei = 100 V.

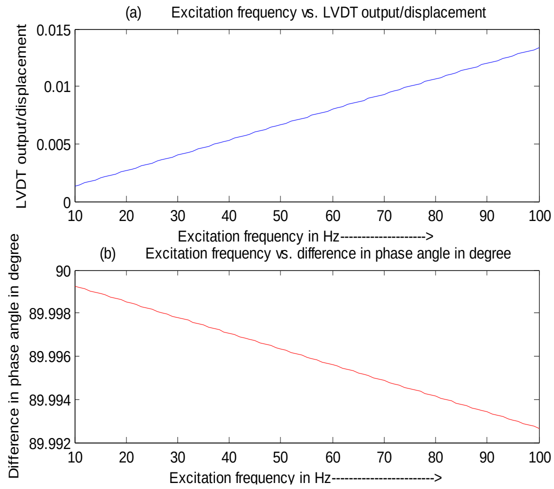

Fig. 2. Variation of output and difference between phase angle with frequency.

From Fig. 2(a), it is clear that $E_o(j\omega)/d(j\omega)$ varies linearly with frequency ‘ω’. Though the variation of the difference in phase angle as shown in Fig. 2(b) is nearly equal to 900, but it varies linearly with ‘ω’. As the displacement increases, since the values of M1 and M2 changes, Eo also changes linearly for a certain displacement and then Eo remains fixed for further displacement on both side. Now as the core moves upward or right direction, the difference of phase angle between the output and the input becomes positive and when it moves downward or left direction, the difference of phase angle become negative. All that have been discussed so far are for the ideal condition of an LVDT, i.e. inter-winding and stray capacitances have not been considered that will be discussed in the next section.

3. WORKING OF LVDT WITH INTER WINDING AND STRAY CAPACITANCES

Fig. 3 shows the equivalent circuit diagram of an LVDT considering the inter-winding and stray capacitances. Here Cp is the equivalent capacitance on the primary side and Cs is that on the secondary side.

Now for the primary side, using KCL, Ei can be written as

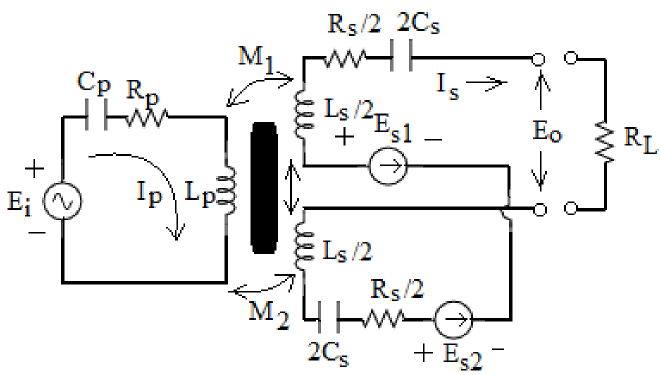

Fig. 3. Equivalent circuit diagram of an LVDT considering the inter-winding and stray capacitance.

Communications on Applied Electronics (CAE) – ISSN : 2394-4714
Foundation of Computer Science FCS, New York, USA
Volume 3– No.6, November 2015 – www.caeaccess.org

$$IpRp + \frac{1}{C_p}\int I_p dt + Lp\frac{dI_p}{dt} + (M2 - M1)\frac{dI_s}{dt} = Ei \quad (5)$$

and for the secondary side

$$Is(Rs + RL) + \frac{1}{C_s}\int I_s dt + Ls\frac{dI_s}{dt} + (M1 - M2)\frac{dI_p}{dt} = 0 \quad (6)$$

Now (5) and (6) can be written as

$$(Rp + \frac{1}{sC_p} + sLp)Ip(s) - (M1 - M2)sIs(s) = Ei(s) \quad (7)$$

and

$$[(Rs+ RL) + \frac{1}{sC_s} + sLs]Is(s) + (M1 - M2)sIp(s) = 0 \quad (8)$$

From (8), $Is(s) = -\frac{(M_1 - M_2)sI_p(s)}{[(R_s + R_L) + \frac{1}{sC_s} + sL_s]}$ (9)

Substituting the value of Is(s) in (6) and rearranging we get

$$Ei(s) = (Rp + \frac{1}{sC_p} + sLp)Ip(s) + \frac{(M_1 - M_2)^2 s^2 I_p(s)}{[(R_s + R_L) + \frac{1}{sC_s} + sL_s]}$$

$$= Ip(s)\Big[R_p(R_s + R_L) + \frac{(R_s + R_L)}{sC_p} + sL_p(R_s + R_L) +$$

RpsCp+1s2CpCs+ LpCs+sLsRp+ LsCp+ s2LpLs+ (M1− M2)2s2/ [Rs+ RL+ 1sCs +sLs]

Now, Eo(s) = RLIs(s)

$$= -\frac{R_L(M_1 - M_2)sI_p(s)}{[(R_s + R_L) + \frac{1}{sC_s} + sL_s]}$$

and (M1 – M2) = Kd(s), where d(s) is the Laplace of the displacement of the core in the field and K is a constant.

Hence,

$$\frac{E_o(s)}{E_i(s)d(s)} = -\frac{R_L Ks}{R_p(R_s+R_L) + \frac{(R_s+R_L)}{s\,C_p} + sL_p(R_s+R_L) + \frac{R_p}{s\,C_p} + \frac{1}{s^2 C_p C_s} + \frac{L_p}{C_s} + sL_p R_p + \frac{L_s}{C_p} + s^2 L_p L_s + (M_1 - M_2)^2 s^2}$$

$$= -\frac{R_L Ks/R_p(R_s+R_L)}{1 + \frac{1}{sC_p R_p} + s\frac{L_p}{R_p} + \frac{1}{sC_p(R_s+R_L)} + \frac{1}{s^2 C_p C_s R_p(R_s+R_L)} + \frac{L_p}{C_s R_p(R_s+R_L)} + \frac{sL_p}{(R_s+R_L)} + \frac{L_s}{C_p R_p(R_s+R_L)} + \frac{s^2 L_p L_s}{R_p(R_s+R_L)} + \frac{(M_1-M_2)^2 s^2}{R_p(R_s+R_L)}}$$

(10)

and this gives

$$\frac{E_o(j\omega)}{E_i(j\omega)d(j\omega)} = -\frac{R_L Ks^3/R_p(R_s+R_L)}{s^2 + \frac{s}{\tau_{cp}} + s^3\tau_{lp} + \frac{s\beta}{\tau_{cp}} + \frac{1}{\tau_{cp}\tau_{csm}} + \frac{s^2\tau_{lp}}{\tau_{csm}} + s^3\tau_{pts} + \frac{s^2\tau_{lsm}}{\tau_{cp}} + s^4\tau_{lp}\tau_{lsm} + s^4\tau_m^2}$$

$$= \frac{R_L Kj\omega^3/R_p(R_s+R_L)}{[\frac{1}{\tau_{cp}\tau_{csm}} - \omega^2(1 + \frac{\tau_{lp}}{\tau_{csm}} + \frac{\tau_{lsm}}{\tau_{cp}}) + \omega^4(\tau_{lp}\tau_{lsm} + \tau_m^2)] + j[\frac{\omega}{\tau_{cp}}(1+\beta) - \omega^3(\tau_{lp} + \tau_{pts})]} \quad (11)$$

where, $\tau_{cp} = C_p R_p, \tau_{lp} = \frac{L_p}{R_p}, \tau_{csm} = C_s(R_s + R_L)$, $\tau_{lsm} = \frac{L_s}{(R_s+R_L)}, \tau_{pts} = \frac{L_p}{(R_s+R_L)}, \beta = \frac{R_p}{(R_s+R_L)}$

and $\tau_m^2 = \frac{(M_1-M_2)^2}{R_p(R_s+R_L)}$

Hence, the magnitude of (11) is

$$A = \left|\frac{E_o(j\omega)}{E_i(j\omega)d(j\omega)}\right| = \frac{R_L K\omega^3/R_p(R_s+R_L)}{\sqrt{[\{\frac{1}{\tau_{cp}\tau_{csm}} - \omega^2\left(1 + \frac{\tau_{lp}}{\tau_{csm}} + \frac{\tau_{lsm}}{\tau_{cp}}\right) + \omega^4(\tau_{lp}\tau_{lsm} + \tau_m^2)\}^2 + \{\frac{\omega}{\tau_{cp}}(1+\beta) - \omega^3(\tau_{lp} + \tau_{pts})\}^2]}} \quad (12)$$

and phase angle between Es and Ei is, $\theta = 90^0 - \tan^{-1}[\frac{\frac{\omega}{\tau_{cp}}(1+\beta) - \omega^3(\tau_{lp} + \tau_{pts})}{\frac{1}{\tau_{cp}\tau_{csm}} - \omega^2\left(1 + \frac{\tau_{lp}}{\tau_{csm}} + \frac{\tau_{lsm}}{\tau_{cp}}\right) + \omega^4(\tau_{lp}\tau_{lsm} + \tau_m^2)}]$ (13)

So the output of the LVDT is given by, EO = AθEid and $|E_0| = A|E_i|d$ (14)

It is seen from (12) and (13) that, both 'A' and 'θ' vary with excitation frequency (ω). The variation of 'A' with 'ω' is shown in Fig. 4 for different values of the constant 'K', i.e. for three different LVDT. From the Fig., it is clear, that the amplitude of the output of LVDT varies nonlinearly with frequency, though it is linear over a small frequency range. Hence if the inter-winding and stray capacitances are considered, the output can be obtained linear for a fixed range of frequency.

Typical ranges of the self and mutual inductances of the LVDT used to draw the plots in Fig.4 are given in Table 1 along with the values of the primary and secondary resistances and capacitances. Though the mutual inductances between the primary and the secondary vary with the core displacement, the values of M1 and M2 mentioned here are for displacement, d = 2 mm.

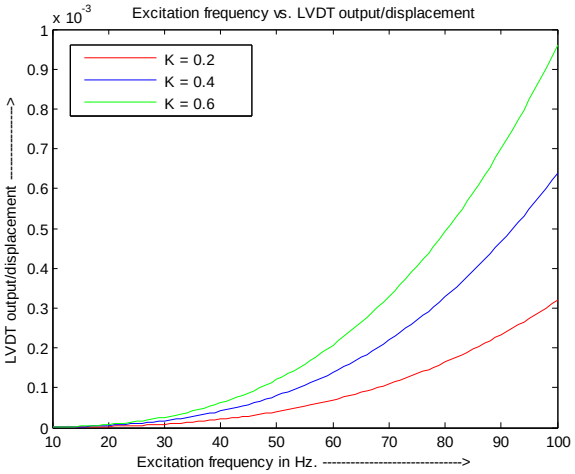

Fig. 4. Variation of 'A' with excitation frequency 'ω'.

Table 1. Typical values of the inductances, resistances and capacitances both for primary and secondary of the LVDT used in the experiment

L_P	M_1	M_2	L_{S1}	L_{S2}	C_P	C_S	R_P	R_S
6 mH	1–8 mH	1–8 mH	2 mH	2 mH	0.2 μF	0.4 μF	100 Ω	150 Ω

From the above table, the values of $\tau_{cp}, \tau_{lp}, \tau_{csm}, \tau_{lsm}, \tau_{pts}$, β and τ_m can be calculated as

Communications on Applied Electronics (CAE) – ISSN : 2394-4714
Foundation of Computer Science FCS, New York, USA
Volume 3– No.6, November 2015 – www.caeaccess.org

shown in Table 2 considering M1= 8 mH, M2 = 4 mH, LS = 4 mH, RL = 200 Ω.

Table 2. Values of different time constants and 'β'

τ_{cp} sec	τ_{lp} sec	τ_{csm} sec	τ_{lsm} sec	τ_{pts} sec	τ_m sec	β
$2e^{-5}$	$6e^{-5}$	$28e^{-5}$	$1.12e^{-5}$	$1.7e^{-5}$	$2.05e^{-5}$	0.28

So the value of A is 3.99x10-8, taking ω = 50 Hz and K = 0.02. Hence the output of the LVDT for 2 mm core displacement is 7.98x100x10-8 = 0.00007 mV, where Ei is taken as 100 V. Fig. 5 shows the LVDT output for different excitation frequency with fixed value of 'd'(2 mm) and 'K'(2). Fig. 6 shows the difference in phase angle for different frequency.

From Fig. 5, it is clear that the difference in phase angle is greater than that obtained without considering the effect of inter-winding and stray capacitance. Hence, if the core moves upward/right direction or downward/left direction, there will be a significant change in phase angle with the input excitation signal. Hence the design of the lead/lag compensator will be more difficult in case if the inter-winding or stray capacitances are considered.

4. EXPERIMENT AND RESULTS

Experiment has been performed by measuring the output with excitation frequency for fixed value of 'd'. Here the displacement (d) is kept constant as 2 mm and the variations of the output for various frequencies are being tabulated in Table 3. The plot corresponding to the results obtained is shown in Fig. 7 where it is compared with the theoretical plot as shown in Fig. 4. It is noticed that the experimental results are nearly similar to the theoretical results as obtained considering the inter-winding and stray capacitances. Also a comparison on the differences of phase angle between input and outputs for different frequencies and for fixed displacement (d = 2 mm) has been studied using CRO and shown in Table 4 and Fig. 8.

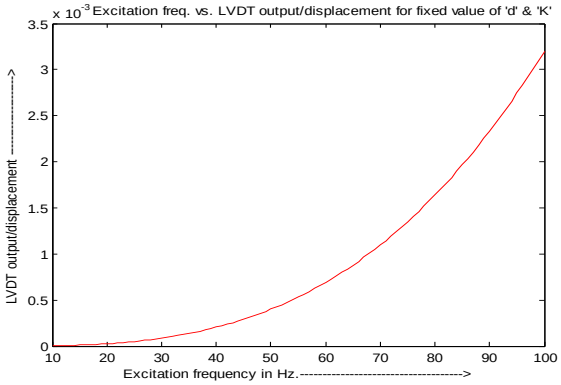

Fig. 5. Variation of LVDT output/displacement with frequency for fixed 'd' and 'K'.

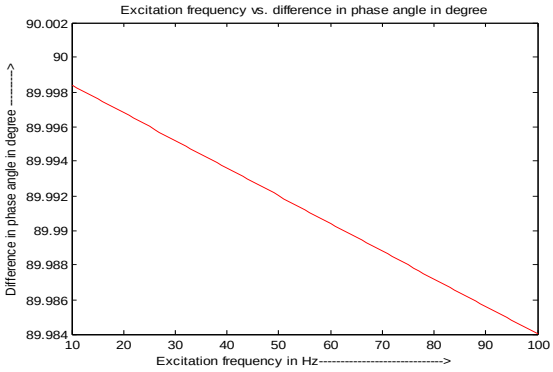

Fig. 6. Difference in phase angle with excitation frequency.

Using equation (12), calculating the parameters ($\tau_{cp}, \tau_{lp}, \tau_{csm}, \tau_{lsm}, \tau_{pts}, \beta$) of the LVDT using the values shown in Table 1 and taking fixed values of 'd'(2 mm), Ei and Eo, the value of τ_m is found out in terms of 'K' . Using this value, the value of (M1 – M2) can be calculated in terms of 'K'. Then using equation (M1 – M2) = Kd, the ratio of M1 and M2 can be calculated and from which, the value of 'K' can be found out which is equal to 2 for M1 and M2 are 8 mH and 4 mH respectively. The plot of the theoretical and practical outputs against excitation frequency for fixed displacement d = 2 mm are shown in Fig. 7 with blue and red color respectively. From the Fig., it is clear that the theoretical curve nearly overlaps with experimental curve.

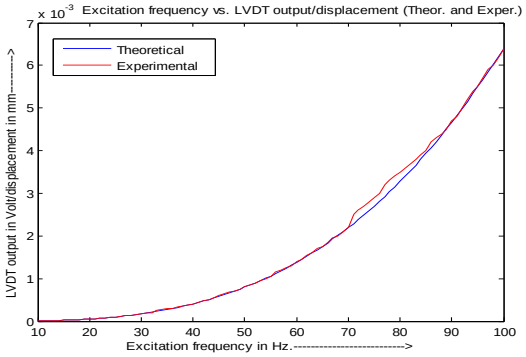

Fig.7. Excitation frequency vs. LVDT output/mm displacement both for theoretical and experimental.

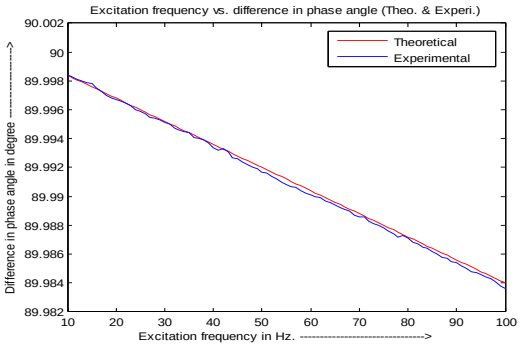

Fig. 8. Differences in phase angle with frequency both for theoretical and experimental.

5. CONCLUSION

From the above discussions and experiment, it is clear that though the output and the phase angle of the output of an LVDT are assumed constant, it is not true for low range measurement. In case of high range measurement, the errors due to inter-winding and stray capacitances can be neglected, but in case low range displacement measurement, the error due to change in excitation frequency is significant, because in that case, the effects of the reactance due to inter-winding and stray capacitances are very much considerable. Since, the results of the experiment show that the output and the difference in phase angle of the output are nearly equivalent, in case of low range measurement, the designer must remember the effect of the unwanted capacitive effects to design lead-lag compensator and the measurement procedure for low range measurement, where accuracy is an important factor, should follow the effects in order to avoid erroneous results.

6. REFERENCES

[1] D. Patranabis, Principles of Industrial Instrumentation (Second Edition), 2000, Tata McGraw-Hill Publication.

[2] L.A. Sharif, M. Kilani, S. Taifour, A. J. Issa, E. A. Qaisi, F. A. Eleiwi and O. N. Kamal, "Linear Variable Differential Transformer Design and Verification using MATLAB and Finite Element Analysis", www.intechopen.com.

[3] U.K. Muhammad, S. Umar, "Sensitivity Determination of Linear Variable Differential Transducer (LVDT) in Fluid Level Detection Techniques", International Journal of Modern Engineering Sciences, vol. 2(2), pp(s). 73 -83, 2013.

[4] D. L. Knudson, J. L. Rempe, "Evaluation of LVDTs for Use in ATR Irradiation Experiments", Sixth American Nuclear Society International Meeting on Nuclear Plant Instrument, Control and Human-Machine Interface Technologies, NPIC&HMIT 2009, Knoxville, Tennessee, April 5-9, 2009, on CD-ROM, American Nuclear Society, LaGrange Park, IL (2009).

[5] Saxena, S.C. and Saksena, S. B. L., "A self compensated smart LVDT transducer", IEEE Trans. Inst. & Meas. Vol. 38 No. 3, 1989, pp. 748-753.

[6] D. J. White, W. A. Take and M. D. Bolton, "Soil deformation measurement using particle image velocimetry (PIV) and photogrammetry," Geotechnique, vol. 53, no. 7, pp. 619-631, 2003.

[7] Pataranabis, D.; Ghosh. S. and Bakshi, C., "Linearining transducer characteristics", IEEE Trans. Inst. & Meas. Vol. IM 37 No. 1, March 1988, pp. 66-6

[8] Holmberg, P., "Automatic balancing of linear ac bridge circuit for capacitive sensor elements", IEEE Trans. Inst. & Meas. Vol. 44 No. 3, June 1995, pp. 803-805

[9] R. Mishra, **"**LVDT: Basic Principle, Theory, Working, Explanation & Diagram - Linear Variable Differential Transformer" July 21, 2012, https://learnprotocols.Wordpress.com/2012/07/21/lvdt-basic-principle-theory-working-explanation-diagr am-linear-variable-differential-transformer/

[10] A. Fuchs, M. J. Moser, H. Zangl and T. Bretterklieber, "Using Capacitive Sensing to Determine the Moisture Content of Wood Pellets – Investigations and Application, International Journal on Smart Sensing and Intelligent Systems, vol. 2, no. 2, June 2009.

[11] M. Soleimani and M. G. Afshar, "Potentiometric Sensor for Trace Level Analysis of Copper Based on Carbon Paste Electrode Modified with Multi-walled Carbon Nanotubes", Int. J. Electrochemical. Sci., vol. 8, pp(s). 8719 – 8729, 2013.

[12] S.V. Thatthachary, B. George and V.J. Kumar, "A resistive potentiometric type transducer with contactless slide, Seventh International Conference on Sensing Technology (ICST), 3-5 December, 2013, pp(s). 501 – 505.

[13] E. O. Doebelin, Measurement Systems-Application & Design, 5th ed. New York: McGraw-Hill, 2004.

[14] S. K. Mishra and G. Panda, "A novel method for designing LVDT and its comparison with conventional design", Proceedings of the 2006 IEEE Sensors Applications Symposium, pp(s). 129-134, 2006.

[15] P. Chellapandi, V. R. Babu, P. Puthiyavinayagam, S. C. Chetal and B. Raj, "Experimental Evaluation of Integrity of FBR Core under Seismic Events", Journal of Power and Energy Systems, vol. 2, No. 2, pp(s). 582 – 589.

[16] P. K. Dhiman, K. Pal and R. K. Sharma, "Strain Gauge Based Displacement Sensor", Journal of Physical Sciences, Vol. 10, 2006, pp(s). 164 – 166.

[17] H. Norton, "Transducer fundamentals," in Handbook of Transducers, Englewood Cliffs, NJ: Prentice Hall, 1989, Ch. 2.

7. APPENDIX

Table 3. Variations of the output for various frequencies

Frequency in Hz.	LVDT output in Volt/mm core displacement (theoretical)	LVDT output in Volt/mm core displacement (practical)	Frequency in Hz.	LVDT output in Volt/mm core displacement (theoretical)	LVDT output in Volt/mm core displacement (practical)
10	$6.4x10^{-6}$	$6.5x10^{-6}$	56	$11.24x10^{-4}$	$11.5x10^{-4}$
11	$8.52x10^{-6}$	$8.8x10^{-6}$	57	$11.85x10^{-4}$	$12x10^{-4}$
12	$11.06x10^{-6}$	$11.1x10^{-6}$	58	$12.48x10^{-4}$	$12.5x10^{-4}$
13	$14.06x10^{-6}$	$14.2x10^{-6}$	59	$13.14x10^{-4}$	$13x10^{-4}$

14	$17.56x10^{-6}$	$17.7x10^{-6}$	60	$13.82x10^{-4}$	$14x10^{-4}$
15	$2.16x10^{-5}$	$2.2x10^{-5}$	61	$14.53x10^{-4}$	$14.5x10^{-4}$
16	$2.62x10^{-5}$	$2.7x10^{-5}$	62	$15.25x10^{-4}$	$15.5x10^{-4}$
17	$3.14x10^{-5}$	$3.2x10^{-5}$	63	$16x10^{-4}$	$16x10^{-4}$
18	$3.73x10^{-5}$	$3.8x10^{-5}$	64	$16.77x10^{-4}$	$17x10^{-4}$
19	$4.39x10^{-5}$	$4.4x10^{-5}$	65	$17.57x10^{-4}$	$17.5x10^{-4}$
20	$5.12x10^{-5}$	$5.2x10^{-5}$	66	$18.39x10^{-4}$	$18.5x10^{-4}$
21	$5.93x10^{-5}$	$6x10^{-5}$	67	$19.24x10^{-4}$	$19.5x10^{-4}$
22	$6.81x10^{-5}$	$7x10^{-5}$	68	$20.12x10^{-4}$	$20x10^{-4}$
23	$7.78x10^{-5}$	$7.9x10^{-5}$	69	$21.02x10^{-4}$	$21x10^{-4}$
24	$8.84x10^{-5}$	$8.9x10^{-5}$	70	$21.95x10^{-4}$	$22x10^{-4}$
25	$9.98x10^{-5}$	$10x10^{-5}$	71	$2.29x10^{-3}$	$2.5x10^{-3}$
26	$11.25x10^{-5}$	$11.5x10^{-5}$	72	$2.39x10^{-3}$	$2.6x10^{-3}$
27	$12.58x10^{-5}$	$12.5x10^{-5}$	73	$2.49x10^{-3}$	$2.7x10^{-3}$
28	$14.04x10^{-5}$	$14x10^{-5}$	74	$2.59x10^{-3}$	$2.8x10^{-3}$
29	$15.6x10^{-5}$	$15.5x10^{-5}$	75	$2.7x10^{-3}$	$2.9x10^{-3}$
30	$17.27x10^{-5}$	$17.5x10^{-5}$	76	$2.81x10^{-3}$	$3x10^{-3}$
31	$19.06x10^{-5}$	$19x10^{-5}$	77	$2.92x10^{-3}$	$3.2x10^{-3}$
32	$2.09x10^{-4}$	$2x10^{-4}$	78	$3.04x10^{-3}$	$3.3x10^{-3}$
33	$2.3x10^{-4}$	$2.5x10^{-4}$	79	$3.15x10^{-3}$	$3.4x10^{-3}$
34	$2.52x10^{-4}$	$2.8x10^{-4}$	80	$3.28x10^{-3}$	$3.5x10^{-3}$
35	$2.74x10^{-4}$	$2.9x10^{-4}$	81	$3.4x10^{-3}$	$3.6x10^{-3}$
36	$2.99x10^{-4}$	$3x10^{-4}$	82	$3.53x10^{-3}$	$3.7x10^{-3}$
37	$3.24x10^{-4}$	$3.3x10^{-4}$	83	$3.66x10^{-3}$	$3.8x10^{-3}$
38	$3.51x10^{-4}$	$3.5x10^{-4}$	84	$3.79x10^{-3}$	$3.9x10^{-3}$
39	$3.79x10^{-4}$	$3.8x10^{-4}$	85	$3.93x10^{-3}$	$4x10^{-3}$
40	$4.09x10^{-4}$	$4x10^{-4}$	86	$4.07x10^{-3}$	$4.2x10^{-3}$
41	$4.41x10^{-4}$	$4.5x10^{-4}$	87	$4.21x10^{-3}$	$4.3x10^{-3}$
42	$4.74x10^{-4}$	$4.8x10^{-4}$	88	$4.36x10^{-3}$	$4.4x10^{-3}$
43	$5.09x10^{-4}$	$5x10^{-4}$	89	$4.51x10^{-3}$	$4.5x10^{-3}$
44	$5.45x10^{-4}$	$5.5x10^{-4}$	90	$4.66x10^{-3}$	$4.7x10^{-3}$
45	$5.83x10^{-4}$	$6x10^{-4}$	91	$4.82x10^{-3}$	$4.8x10^{-3}$
46	$6.23x10^{-4}$	$6.4x10^{-4}$	92	$4.98x10^{-3}$	$5x10^{-3}$
47	$6.64x10^{-4}$	$6.8x10^{-4}$	93	$5.15x10^{-3}$	$5.2x10^{-3}$
48	$7.08x10^{-4}$	$7x10^{-4}$	94	$5.36x10^{-3}$	$5.4x10^{-3}$
49	$7.53x10^{-4}$	$7.5x10^{-4}$	95	$5.49x10^{-3}$	$5.5x10^{-3}$
50	$7.99x10^{-4}$	$8x10^{-4}$	96	$5.66x10^{-3}$	$5.7x10^{-3}$
51	$8.49x10^{-4}$	$8.5x10^{-4}$	97	$5.84x10^{-3}$	$5.9x10^{-3}$
52	$8.99x10^{-4}$	$9x10^{-4}$	98	$6.02x10^{-3}$	$6x10^{-3}$
53	$9.53x10^{-4}$	$9.5x10^{-4}$	99	$6.21x10^{-3}$	$6.2x10^{-3}$
54	$10.07x10^{-4}$	$10x10^{-4}$	100	$6.39x10^{-3}$	$6.4x10^{-3}$
55	$10.64x10^{-4}$	$10.5x10^{-4}$	101	$6.5x10^{-3}$	$6.6x10^{-3}$

Table 4. **Differences in phase angle with frequency (theoretical and experimental)**

Frequency in Hz.	Difference in phase angle in degree (Theoretical)	Difference in phase angle in degree (Experimental)	Frequency in Hz.	Difference in phase angle in degree (Theoretical)	Difference in phase angle in degree (Experimental)
10	89.9984000007253	89.9984	56	89.9908801343222	89.9907
11	89.9982400009654	89.9983	57	89.9907201415164	89.9906
12	89.9980800012534	89.9981	58	89.9905601489629	89.9904
13	89.9979200015936	89.998	59	89.9904001566662	89.9902
14	89.9977600019903	89.9979	60	89.9902401646306	89.9901
15	89.9976000024480	89.9978	61	89.9900801728605	89.99
16	89.9974400029710	89.9975	62	89.9899201813601	89.9899
17	89.9972800035636	89.9973	63	89.9897601901338	89.9897
18	89.9971200042301,	89.997	64	89.9896001991861	89.9896
19	89.9969600049750	89.9968	65	89.9894402085212	89.9894
20	89.9968000058026	89.9967	66	89.9892802181434	89.9892
21	89.9966400067173	89.9966	67	89.9891202280573	89.9891
22	89.9964800077233	89.9965	68	89.9889602382670	89.989
23	89.9963200088251	89.9963	69	89.9888002487769	89.9887

24	89.9961600100270	89.996	70	89.9886402595914	89.9886
25	89.9960000113333	89.9959	71	89.9884802707149	89.9886
26	89.9958400127484	89.9957	72	89.9883202821517	89.9883
27	89.9956800142766	89.9955	73	89.9881602939061	89.9881
28	89.9955200159224	89.9954	74	89.9880003059824	89.988
29	89.9953600176900	89.9953	75	89.9880003059824	89.9878
30	89.9952000195838	89.9951	76	89.9878403183852	89.9876
31	89.9950400216082	89.995	77	89.9876803311186	89.9874
32	89.9948800237675	89.9947	78	89.9875203441870	89.9872
33	89.9947200260660	89.9946	79	89.9873603575948	89.9873
34	89.9944000310983	89.9945	80	89.9872003713464	89.9871
35	89.9942400338407	89.9944	81	89.9870403854461	89.9868
36	89.9940800367398	89.9941	82	89.9868803998981	89.9867
37	89.9939200397999	89.994	83	89.9867204147070	89.9865
38	89.9937600430254	89.9939	84	89.9865604298770	89.9864
39	89.9936000464206	89.9937	85	89.9864004454125	89.9862
40	89.9934400499898	89.9934	86	89.9862404613178	89.986
41	89.9932800537375	89.9932	87	89.9860804775973	89.9858
42	89.9931200576680	89.9933	88	89.9859204942553	89.9857
43	89.9929600617856	89.9931	89	89.9857605112962	89.9855
44	89.9928000660946	89.9927	90	89.9856005287243	89.9854
45	89.9926400705995	89.9926	91	89.9854405465440	89.9852
46	89.9924800753046	89.9924	92	89.9852805647596	89.985
47	89.9923200802142	89.9922	93	89.9851205833755	89.9848
48	89.9921600853327	89.992	94	89.9849606023959	89.9847
49	89.9920000906644	89.9919	95	89.9848006218254	89.9846
50	89.9918400962136	89.9917	96	89.9846406416682	89.9844
51	89.9916801019849	89.9916	97	89.9844806619286	89.9843
52	89.9915201079824	89.9914	98	89.9843206826110	89.9841
53	89.9913601142105	89.9912	99	89.9841607037198	89.9838
54	89.9912001206736	89.991	100	89.9840007252593	89.9836
55	89.9910401273761	89.9908	101	89.983912532134	89.9832